JPP Journal of Pharmacy and Pharmacology

JPP 2003, 55: 495–504

Received July 18, 2002
Accepted January 16, 2003
DOI 10.1211/002235702847
ISSN 0022-3573

Direct, differential-equation-based in-vitro–in-vivo correlation (IVIVC) method

Peter Buchwald

Abstract

A new, differential equation-based in-vitro–in-vivo correlation (IVIVC) method is proposed that directly relates the time-profiles of in-vitro dissolution rates and in-vivo plasma concentrations by using one- or multi-compartment pharmacokinetic models and a corresponding system of differential equations. The rate of in-vivo input is connected to the rate of in-vitro dissolution through a general functional dependency that allows for time scaling and time shifting. A multiplying factor that accounts for the variability of absorption conditions as the drug moves along is also incorporated. Two data sets incorporating slow-, medium-, and fast-release formulations were used to test the applicability of the method, and predictive powers were assessed with a leave-one-formulation-out approach. All fitted parameters had realistic values, and good or acceptable fits and predictions were obtained as measured by plasma concentration mean squared errors and percent AUC errors. Introduction of step-down functions that account for the transit of the dosage form past the intestinal sites of absorption proved useful. By avoiding the integral transforms used in the existing deconvolution- or convolution-based IVIVC models, the present method can provide increased transparency, improved performance, and greater modelling flexibility.

Introduction

In-vitro–in-vivo correlation (IVIVC) methods are increasingly used in the development of extended-release dosage forms and are now FDA-regulated (US Department of Health and Human Services, Food and Drug Administration, Center for Drug Evaluation and Research (CDER) 1997). Such methods aim to establish quantitative, reproducible relationships between some easily measurable in-vitro characteristics of a dosage form, such as the in-vitro dissolution rate, and in-vivo biological parameters of interest that are considerably more time- and labour-expensive to obtain. These could be simple parameters such as C_{max}, t_{max} or AUC; however, the ultimate goal is a predictive model connecting the time course of relevant in-vivo pharmacokinetic parameters to the time course of the in-vitro release (so-called Level A models). Current FDA regulations (US Department of Health and Human Services, Food and Drug Administration, Center for Drug Evaluation and Research (CDER) 1997) state that "Whatever the method used to establish a Level A IVIVC, the model should predict the entire in-vivo time course from the in-vitro data. In this context, the model refers to the relationship between in-vitro dissolution of an ER dosage form and an in-vivo response such as plasma drug concentration or amount of drug absorbed."

Indeed, the time course of plasma concentration, C(t), which is in fact the directly measured and the pharmacokinetically most relevant parameter, should be the predictive target of such methods, as it is increasingly happening in recent publications (Gillespie 1997; Eddington et al 1998; Modi et al 2000; Sirisuth & Eddington 2000; Veng-Pedersen et al 2000; Dalton et al 2001; O'Hara et al 2001; Pitsiu et al 2001). Nevertheless, FDA regulations, in agreement with most of the older literature, focus on so-called deconvolution-based methods and mention only one alternative method, the more recently introduced so-called convolution-based method (Gillespie 1997; Veng-Pedersen et al 2000). This paper describes a different approach using a direct, differential-equation-based IVIVC method. Most basic assumptions of this method are

IVAX Research, Inc.,
4400 Biscayne Blvd., Miami,
Florida 33137, USA

Peter Buchwald

Correspondence: P. Buchwald, IVAX Research, Inc., 4400 Biscayne Blvd., Miami, Florida 33137, USA.
E-mail: Peter_Buchwald@ivax.com

essentially the same as those of the other two methods. However, by relying on the (numeric) solution of the differential equations resulting from clear pharmacokinetic-type models, the need for integral transforms is avoided and much more flexible and transparent models are obtained.

Deconvolution-based IVIVC methods

These methods are two-stage modelling procedures. In the first stage, a deconvolution method is used to estimate the time course of in-vivo absorption (fraction absorbed f_{abs} vs time t). The deconvolution methods used, such as the Wagner–Nelson (Wagner & Nelson 1963), Loo–Riegelman (Loo & Riegelman 1968) or general non-compartmental methods, involve many (often tacit or overlooked) assumptions (Wagner 1975; Gibaldi & Perrier 1982) to deal with the underlying pharmacokinetic model as well as rough numerical estimates (Wang & Nedelman 2002) to deal with the mathematical difficulties of the deconvolution. In the second stage, the in-vivo absorption (or release) time profile obtained in this first stage is connected to the time course of the in-vitro dissolution profile. Usually a point-to-point relationship is established between the in-vivo and in-vitro parameters of the same time point (e.g., in-vivo fraction absorbed f_{abs} vs in-vitro fraction dissolved f_{dis}); most commonly, one described by a simple linear function, sometimes by others, for example, sigmoidal, Hill-type functions. Attempts to establish simple linear relationships between f_{abs} and f_{dis} can probably be traced back to the original and very narrow definition of level A correlations: the in-vitro and in-vivo dissolution curves are superimposable. These methods allow for only very limited modelling flexibility and are difficult to use for plasma concentration estimates.

Convolution-based IVIVC methods

Contrary to the previous case, convolution-based methods are one-stage modelling approaches, and they directly relate the time course of the in-vivo measured plasma concentration to the time profile of the in-vitro dissolution. The equation that forms the basis of these approaches (Gillespie 1997; Modi et al 2000; Veng-Pedersen et al 2000; Balan et al 2001; O'Hara et al 2001; Pitsiu et al 2001; Gomeni et al 2002) relies on a convolution-type (Riley et al 1997) integral transform:

$$C(t) = r(t) * C_\delta(t) = \int_0^t C_\delta(t-\tau)r(\tau)d\tau \qquad (1)$$

Here, C is the plasma concentration, r is the in-vivo input (absorption) rate and C_δ is a so-called unit impulse response, which corresponds to the plasma concentration profile resulting from the instantaneous in-vivo release (absorption) of a unit amount of drug. Such convolutions, which are denoted with the * symbol, are commutative

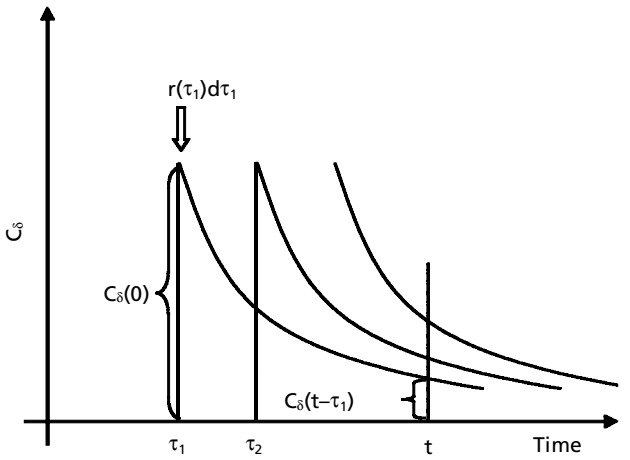

Figure 1 Rationale for convolution-based IVIVC models. The plasma concentration resulting from each infinitesimal input $r(\tau)d\tau$ decreases following the unit impulse response C_δ curve. The total concentration C(t) at time t is the sum (integral) of all the remaining fractions $C_\delta(t-\tau)$ of the infinitesimal contributions $r(\tau)d\tau$ made at time τ (equation 1).

($r^*C_\delta = C_\delta^*r$), associative and distributive. Figure 1 illustrates the rationale for this equation. At any time point τ, a drug (concentration) amount of $r(\tau)d\tau$ is released (absorbed). The corresponding unit plasma concentration decreases following the C_δ time profile as shown for τ_1 and τ_2 in Figure 1. At a later time point t, a $t-\tau$ time passed, and the remaining drug (concentration) amount from this release is $r(\tau)d\tau$ times the remaining unit value, hence, $C_\delta(t-\tau)r(\tau)d\tau$. The total plasma concentration at time t, C(t), is obtained by summing up all the infinitesimal contributions of all earlier time-points τ (i.e., integrating on τ from 0 to t), which results in equation 1.

If a concentration profile following intravenous administration is not available to obtain C_δ, then a sum of exponential functions (corresponding to linear pharmacokinetic models and first-order eliminations) is usually employed:

$$C_\delta(t) = \sum_j A_j e^{-\alpha_j t} \qquad (2)$$

The corresponding coefficients (A_j, α_j) are obtained by fitting (e.g., on a terminal elimination phase when the input process is negligible). Within this context, establishing an IVIVC comes downs to establishing the functional dependence f that relates the in-vivo input (release or absorption) rate to the in-vitro dissolution rate, $r_{dis}(t)$

$$r = f(r_{dis}, t) \qquad (3)$$

The simplest choice is a linear one

$$r(t) = a_0 + a_1 r_{dis}(t) \qquad (4)$$

The identity $r(t) = r_{dis}(t)$, which corresponds to $a_0 = 0$, $a_1 = 1$, is the most trivial possibility and represents the so-called basic convolution-based IVIVC method (Gillespie 1997). Time scaling is also frequently justifiable:

$$r(t) = s_r r_{dis}(t_0 + s_1 t) \qquad (5)$$

Here, s_1 is the time-scaling factor, and a scaling factor s_r was also included; this allows amplitude scaling and also absorbs differences in units of measurements. Equation 5 assumes that the time profiles of the in-vitro and in-vivo release are similar, but they are compressed or expanded compared with each other. Indeed, the two release rates may operate on different time scales (e.g., due to different agitation conditions (Brockmeier et al 1985)). The presence of a slight time-delay (time-shift or lag time, $t_0 \leq 0$) for the in-vivo data is also a realistic assumption in most cases, because compared with the in-vitro case in which dissolution starts instantaneously, in-vivo absorption (appearance of C) may be somewhat delayed. It may be particularly so if absorption in the stomach is limited (e.g., by an acid-resistant coating or by the nature of the compound). Many other functional dependencies may be employed for equation 3, if they are justifiable. Obviously, by including a sufficiently large number of parameters and functional dependencies, various time profiles can be fitted, but the final model should result from justifiable selections that are based both on mechanism-related knowledge and on the goodness of fit and prediction.

Direct, differential-equation-based IVIVC method

The method proposed here is also a one-stage method and in many ways similar to convolution-based methods. However, instead of using integral transforms such as those described by equation 1, the corresponding differential equations that result from the underlying pharmacokinetic model are solved directly. This is a much more obvious choice, and the corresponding numeric solutions can be easily performed by using a variety of approaches or softwares. Basic assumptions are summarized in Figure 2.

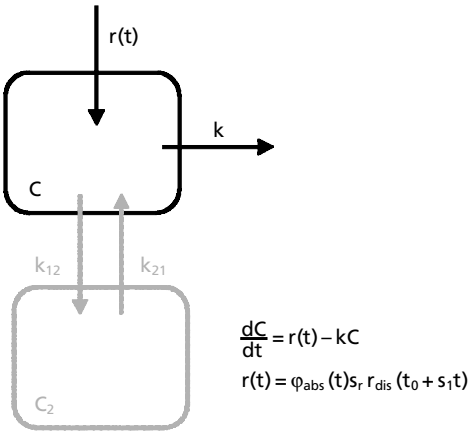

Figure 2 Basic assumptions of the present direct, differential-equation-based IVIVC method. It corresponds to the usual one- or two-compartment pharmacokinetic model, but the rate of in-vivo input r is connected to the rate of in vitro dissolution r_{dis} through the functional dependency shown.

Distribution/elimination is assumed to take place according to usual compartment-based pharmacokinetic models, but with a generalized input rate r and elimination constant k. A one-compartment model can be used as a starting point (to avoid overparametrization), but two- or more-compartment models can be easily accommodated. The elimination constant of this model (k, Figure 2) does not necessarily have to be a fixed constant; any (justifiable) time dependence k(t) can be included in the corresponding differential equation (e.g., Gompertz kinetics in which the rate coefficients are allowed to change exponentially (Easton 2002)). The assumption of one- or two-compartment open models does not introduce any serious limitation compared with the previous methods. The Wagner–Nelson method most frequently used for deconvolution approaches is also based on one-compartment models (Wagner 1975). The exponential-type (equation 2) unit impulse response functions usually used in convolution-based approaches also result from similar models. It is also true, however, that for the present method a particular compartmental model of a specific structure has to be assumed, whereas convolution-based approaches do not assume any particular underlying compartmental model.

Therefore, within the framework of the present model (Figure 2), in-vivo plasma concentration is described by the following differential equation (one-compartment approximation):

$$dC/dt = r(t) - kC \tag{6}$$

with r(t) being connected to $r_{dis}(t)$ through an equation such as equation 3. The input rate r here refers to concentration; therefore, it is in concentration per time units. Hence, compared with the usual drug input rates, a volume term was also incorporated within it. It is also easy to recognize, that with a constant input rate, $r(t) = r_0/V$, the model represents the one-compartment open model with constant rate intravenous infusion, for which the analytical solution of the differential equation (equation 6) is easily available, and the corresponding solution is well-known and widely used (Wagner 1975).

$$r(t) = \frac{r_0}{V} \quad \Rightarrow \quad C = \frac{r_0}{kV}(1 - e^{-kt}) \tag{7}$$

The constant input rate was denoted as r_0/V, where V is a volume term, to maintain similarity with the usual pharmacokinetic notation. Similarly, with an exponentially decreasing input that has an absorption rate constant κ, $r(t) = r_0 e^{-\kappa t}/V = \kappa D_0 e^{-\kappa t}/V$, the model represents the one-compartment open model with first-order absorption, which also has a well-known and widely used analytical solution:

$$r(t) = \frac{r_0}{V} e^{-\kappa t} = \frac{\kappa D_0}{V} e^{-\kappa t} \Rightarrow C = \frac{r_0 \quad \kappa}{\kappa V \kappa - k}(e^{-kt} - e^{-\kappa t}) \tag{8}$$

However, to obtain an IVIVC, the in-vivo drug input (release/absorption) rate, r(t), of the present model (Figure 2) will be connected to the in-vitro drug release (dissolution) rate, $r_{dis}(t)$, through a general functional dependence, just as it was done for the case of the generalized convolution-based methods (equation 3). Of course, it has

to be assumed that, for the formulations and compounds modelled, mainly drug release and not absorption is rate limiting. The model explored here, in addition to time scaling and time shifting (equation 5), also incorporates a time-dependent multiplying factor φ_{abs} that accounts for the variability of the in-vivo absorption conditions as the drug moves along the gastrointestinal tract:

$$r(t) = \varphi_{abs}(t) s_r r_{dis}(t_0 + s_1 t) \tag{9}$$

For example, by incorporating some truncating functions, such as a simple, square step-down ($\varphi_{abs}(t) = 1$ if $t \leq t_{cut}$, $\varphi_{abs}(t) = 0$ if $t > t_{cut}$) or a smoother, sigmoidal step-down ($\varphi_{abs}(t) = e^{-\eta(t - t_{cut})}/(1 + e^{-\eta(t - t_{cut})})$) function, one can account for the transit of the extended-release dosage form past the intestinal sites of absorption. In this work, incorporation of such cut-off functions was found to provide considerable improvement in the quality of the IVIVC models explored. Here, η is just a measure of how steep the cut-off is, and could be used as an adjustable parameter. In this work, a fixed value of $\eta = 10$ was used to keep the number of adjustable parameters to a minimum. Small intestine is the main site of absorption, and the mean small-intestinal transit time of dosage forms is in the range of 3 (± 1) h (Davis et al 1986; Yu & Amidon 1999; Wilding 2000; Agoram et al 2001). Hence, even if one considers the extremely varying gastric emptying time of pharmaceutical dosage forms, in most cases, no considerable systemic absorption from the gastrointestinal tract can be expected 4–10 h after administration unless there is still good absorption from the colon, which may be a possibility for some high-permeability drugs.

With the present model, the IVIVC approach is clearly placed in a pharmacokinetic framework, and there are no convoluted details. It is somewhat surprising that this IVIVC approach, which is the most obvious and straightforward from a pharmacokinetic perspective, has been overlooked until now. Complex sets of differential equations have been used recently in the so-called compartmental absorption and transit (CAT) (Yu & Amidon 1999) and advanced compartmental absorption and transit (ACAT) (Agoram et al 2001) models for oral absorption. However, these are overly complex models (e.g., ACAT allows for 6 drug states, 18 compartments, 3 states of excreted material and up to 3 pharmacokinetic compartments, resulting in a set of approximately 80 coupled ordinary differential equations) and, hence, not easily suitable for transparent and parsimonious IVIVC connections such as equation 9 here.

In the previous paragraphs, only the one-compartment open model was discussed, but extension to two- or multi-compartment open models is self-evident, as denoted with the gray addition in Figure 2. The corresponding equations for a two-compartment case with central compartment elimination are:

$$\begin{cases} \dfrac{dC}{dt} = r(t) - kC - k_{12}C + k_{21}C_2 \\ \dfrac{dC_2}{dt} = k_{12}C - k_{21}C_2 \\ r(t) = \varphi_{abs}(t) s_r r_{dis}(t_0 + s_1 t) \end{cases} \tag{10}$$

To (numerically) solve equations 7 + 9 or 10, values of the dissolution rate r_{dis} are needed at various time points. This, however, can be obtained easily by fitting some model function on the available experimental dissolution data (usually f_{dis}). Depending on the shape of this profile, various functions can be explored. For example, sigmoidal, Hill-type functions (Eddington et al 1998)

$$f_{dis}(t) = F_{max} \frac{t^n}{t_{50}^n + t^n} \tag{11}$$

and exponential, Weibull-type functions (Sathe et al 1997)

$$f_{dis}(t) = F_{max} \left(1 - e^{-\left(\frac{t}{t_{63.2}}\right)^{\beta}} \right) \tag{12}$$

usually provide good fits. Other functions, such as probit, logistic or quadratic functions (Sathe et al 1997; Gabrielsson & Weiner 2000; Costa & Lobo 2001), may also be explored. Eventually, a smooth interpolant such as a cubic spline can also be used. The rate of dissolution can then easily be obtained as the (analytical) derivative of these functions; for example, the sigmoidal function of equation 11 results in

$$r_{dis}(t) = \frac{df_{dis}}{dt} = \frac{n F_{max}\, t_{50}^n\, t^{n-1}}{(t_{50}^n + t^n)^2} \tag{13}$$

By using direct numeric solution to differential equation-based models, the need for a convolution or deconvolution step is eliminated. Furthermore, directly measurable plasma concentrations are directly related to in-vitro measurable fraction-dissolved data through clear models (Figure 2) and corresponding assumptions. The obtained rate of elimination k provides a possibility to verify the correctness of the assumptions used, because it should be close to the usual rate of elimination of the compound. The scaling factors, as well as the time-shift and absorption cut-off parameters, also should have realistic values.

Materials and Methods

Data used to demonstrate the applicability of the method were simulated data. However, they were generated so as to reproduce as closely as possible the diltiazem data of Gillespie (Gillespie 1997) and the metformin data of Balan and co-workers (Balan et al 2001) from the corresponding IVIVC publications. Fraction dissolved profiles were fitted by sigmoidal functions (equation 11, $F_{max} = 100$). Numeric integration of the differential equations (equation 10) were performed in MS Excel by using a simple Euler method and a step size of 0.1 h. Implementation of a smaller step size (0.05 h) provided no significant improvement. Therefore, a step size of 0.1 h was considered as sufficient for our purposes. Runge-Kutta methods (Riley et al 1997) were also explored in a few cases. Parameter fittings were performed by minimizing the sum of squared errors compared with the available experimental C data with the Solver tool of Excel. Fitting was done in a stepwise manner, first fitting only k and s_r and using fixed

values for the other parameters ($s_1 = 1$, $t_{cut} = \infty$, $t_0 = 0$), and then allowing these parameters to vary too. A number of different starting values were used in each case to avoid getting trapped in local minima. Using a standard spreadsheet-based approach is a somewhat simplistic, but sufficiently accurate, approach. A major advantage is that MS Excel is widely available and well suited for such applications or other applications involving quantitative modeling (Buchwald & Bodor 1999, 2000, 2001; Buchwald 2002). Papers describing its applications to deconvolution-based IVIVC methods have been recently published (Langenbucher 2002). To ensure accuracy and error-free models, calculations were also performed using Scientist 2.01 (MicroMath Scientific Software, Salt Lake City, UT) and WinNonlin standard edition 2.1 (Pharsight Corporation, Palo Alto, CA). Unweighted data were used. Model files used are attached in Appendixes 1 and 2. Essentially identical results were obtained in all verified cases; however, Scientist provided considerably slower and less efficient optimizations than Excel's Solver or WinNonlin. Equations were written for the two-compartment model (equation 10), but in both cases the one-compartment model was tested first by fixing $k_{12} = k_{21} = 0$ to minimize the number of adjustable parameters during the exploration phase.

Results and Discussion

To test the present IVIVC method, calculations were performed on two sets of simulated data that were generated so as to reproduce as closely as possible the diltiazem data of Gillespie (Gillespie 1997) and the metformin data of Balan and co-workers (Balan et al 2001) from the corresponding IVIVC publications. Both cases include data for slow-, medium- and fast- release formulations, and also for an immediate-release formulation.

For the diltiazem data (Figures 3 and 4), good fit could be obtained for all three formulations with a combined one-compartment model. Even predictions using a leave-one-out procedure for the three formulations were satisfactory. Sigmoidal functions (equation 11, $F_{max} = 100$) gave reasonably good fit for the three different dissolution profiles (slow, medium and fast). A common, combined model (equation 9 with k, s_r, s_1, t_0 and t_{cut} as adjustable parameters) was then used to simultaneously fit all three in-vivo plasma concentration profiles. That is, the plasma profiles of the individual formulations were not fitted separately, but all three of them (C_f, C_m, and C_s) were simultaneously fit by a single set of five parameters.

Table 1 shows the changes in plasma concentration mean squared errors (MSE) during the stepwise fitting of the parameters. As these data indicate, the model is stable: parameter values stay within well-defined ranges during the various fitting procedures indicating that they have meaningful values. The model is also sufficiently parsimonious by usual statistical measures: five adjustable parameters are used to fit a total of $3 \times 18 = 54$ concentration data points. As the corresponding MSE values indicate, there was no significant need for time scaling; $s_1 = 1$ already gave good fit (fixing $s_1 = 1$ increase the MSE from 3.58 to 4.28 only). The final value obtained by fitting, $s_1 = 1.25$, represents only a relatively small scaling. However, introduction of a time delay $t_0 = -0.71/1.25 = -0.57$ h for the in-vivo data provided considerable improvement (MSE of 3.58 vs 5.46), and the obtained t_0 value is in a very realistic range. Here, because of the way equation 9 was defined, a division by s_1 (1.25) is needed to bring t_0 and t to the same scale. An even more significant improvement (especially for the slow formulation) was obtained by introduction of a sigmoidal-type cut-off φ_{abs} profile with a t_{cut} value of approx. 6.4 h (MSE of 3.58 vs 6.63; Table 1). Again, as mentioned in the introduction, such a value somewhere in the 4–9 h range is very realistic, and it accounts for the transit of the extended-release dosage form past the intestinal sites of absorption. A compensating error in the calculated AUC values causes an apparent increase in prediction error for these values

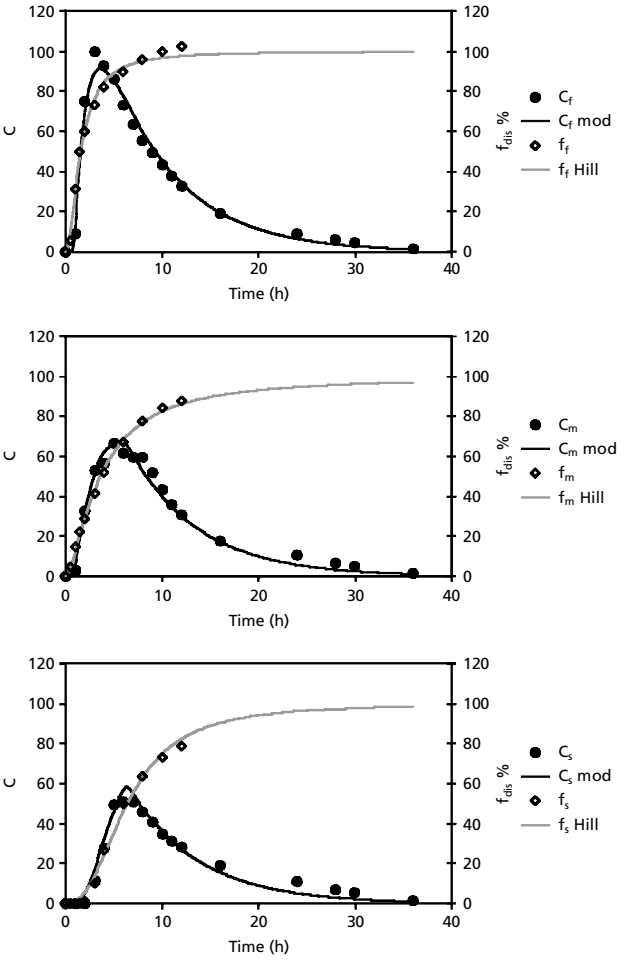

Figure 3 Fraction dissolved (f_{dis}, right vertical axis, open diamond-shaped symbols) and plasma concentration (C, left vertical axis, filled circle-shaped symbols) time profiles for the fast- (f_f, C_f), medium- (f_m, C_m) and slow (f_s, C_s)-release formulations based on the diltiazem data. Lines denote the fitted sigmoidal (Hill)-type dissolution profile and the predicted plasma concentration by the present model fitted simultaneously on all three data.

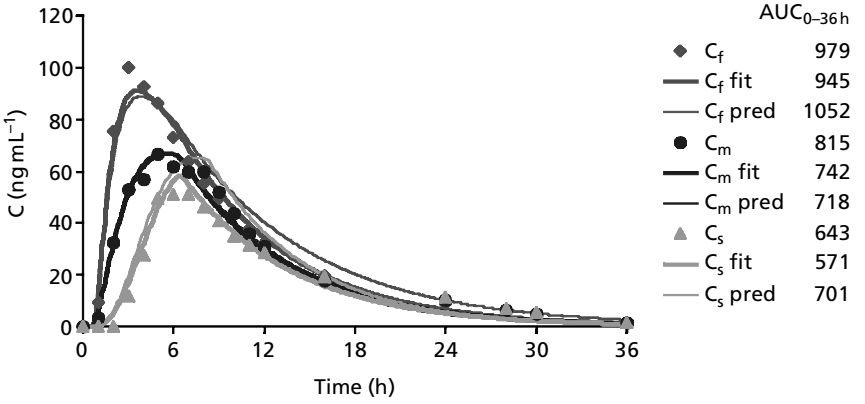

Figure 4 Plasma concentration–time profiles for the diltiazem data. C_f, C_m, and C_s denote values for the fast-, medium- and slow-release formulations, respectively. Experimental data are shown together with predicted values from the present IVIVC method. Thicker lines (C fit) denote predictions of the model fitted simultaneously on all three formulations ($k = 0.138$, $s_r = 1.74$, $s_1 = 1.24$, $t_0 = -0.71$, $t_{cut} = 6.36$), and thinner lines (C pred) denote predicted values for each formulation by the model fitted on the other two formulations (leave-one-out predictions).

(ΔAUC %; Table 1), as the slow formulation is strongly-over-predicted if no t_{cut} is used. For the final model, the Akaike Information Criteria (AIC), a measure of goodness of fit based on maximum likelihood, computed by WinNonlin was 363.2 and the model selection criteria (computed by Scientist) was 3.82. It is also important to note that the value of the elimination constant obtained here by fitting the model, $k = 0.138$, is in excellent agreement with the value of the elimination constant obtained from the immediate-release solution data for the t = 5- to 24-h period, $k = 0.138$ ($n = 5$, $r^2 = 0.96$). This corresponds to a half-life of 5 h that agrees well with literature values. For the same period, elimination of the extended-release formulation is also linear on a log scale and has about the same slope. Introduction of a two-compartment model provided no significant improvement over the one-compartment model.

The predictive power was estimated by using a leave-one-formulation-out procedure: two concentration profiles were used to fit the five-parameter model (k, s_r, s_1, t_0 and t_{cut} adjustable), which then was used to predict the third concentration profile from the corresponding dissolution data. As shown in Figure 4, quite reliable predictions were obtained in this case. As it should be with any well-parameterized predictive model, the best and most consistent profile prediction was obtained for the medium-release formulation, which is between the slow and fast formulations. Predictions outside the fitting range (e.g., predicting slow based on fitting for medium and fast) were less good, the least reliable being that for the slow formulation (Figure 4) (mainly because t_{cut} was not correctly adjusted). $AUC_{0-36\,h}$ values were calculated to characterize the goodness of fit or prediction (Figure 4). Differences compared with experimental values are under 12% for all formulations, including fitted and leave-one-out predictions. These data show that the proposed IVIVC method can provide good predictions, while all

Table 1 Plasma concentration mean squared errors and model selection criteria for fitting of various models for the diltiazem data.

k	0.174	0.211	0.195	0.132	0.142	0.160	0.138
s_r	1.480	1.468	1.849	1.418	1.399	1.576	1.743
s_1	**1**	0.832	1.217	**1**	0.940	**1**	1.245
t_0	**0**	**0**	− 0.779	**0**	**0**	− 0.399	− 0.714
t_{cut}	**50**	**50**	**50**	6.785	7.133	7.191	6.364
MSCrit	2.27	2.31	2.65	2.96	2.95	3.51	3.82
AUC_{f+m+s}	2477	2426	2296	2319	2261	2145	2259
ΔAUC %	1.6	− 0.4	− 5.8	− 4.9	− 7.2	− 12.0	− 7.3
MSE_f	8.96	7.66	5.83	7.84	7.50	4.86	3.97
MSE_m	4.75	4.46	2.91	4.06	3.93	3.47	3.34
MSE_s	9.72	10.31	9.46	3.65	4.19	4.39	3.38
MSE_{all}	8.11	7.85	6.63	5.51	5.46	4.28	3.58

Parameter values denoted in bold were fixed during the corresponding fit. Model selection criteria (MSCrit) were calculated by Scientist at the given parameter values. Changes in the plasma concentration mean squared errors (MSE) are shown separately for each of the three formulations (MSE_f, MSE_m, MSE_s). Total predicted AUCs for the three formulations are also shown together with the corresponding percent prediction errors (ΔAUC %).

of its fitted parameters are in very realistic ranges. With this model, it is also very easy to explore the influence of changing any of the parameters or to calculate predicted plasma concentrations for a new dissolution profile.

The metformin data were somewhat more difficult to fit. However, this is not surprising. Metformin qualifies as a high-solubility, low-permeability compound within the framework of the proposed (Amidon et al 1995) Biopharmaceutical Classification System for drugs, and IVIVC models may not be feasible for such drugs. By most indications, the in-vivo input of metformin in humans is absorption limited (Balan et al 2001). Furthermore, the absorption of metformin from the human gastrointestinal tract is site-dependent with poor or negligible absorption from the stomach and the colon (Vidon et al 1988; Balan et al 2001). In the original IVIVC work, it was not possible to develop a deconvolution-based level A IVIVC model, and an extended convolution-based model could be developed only by using in-vivo input from deconvolution and incorporating in-vivo absorption profiles for individual formulations in the model (which, however, makes for no true in-vitro → in-vivo method) (Balan et al 2001).

With this model, very good individual fits could be achieved for the individual formulations considered separately (not shown), and it was also possible to develop a fitted common model of acceptable quality for the three formulations considered together, $n = 3 \times 17 = 51$ data points (Figure 5). Again, introduction of a time-delay t_0 and a cut-off time t_{cut} improved the model considerably. This is not surprising, as the former can account for the limited absorption from the stomach, and the second for the limited absorption from the colon. Furthermore, additional improvement in fit could be obtained for the fast formulation by introduction of a limiting input rate, r_{max}. If at any time during the integration of equation 6 the in-vivo input rate estimated from equation 9 exceeded this r_{max} value, only the limiting r_{max} was used in the corresponding integration step. Such a limiting r_{max} seemed to account well for the possibility that the in-vivo input of metformin may be absorption limited.

Because a relatively large number of parameters had to be fitted, optimization had to be done somewhat more carefully as the same overall minima could not always be found. The best fit (as judged based on the sum of squared errors) was obtained with the following set of parameters: $k = 0.230$, $s_r = 20.49$, $s_l = 0.58$, $t_0 = -0.50$, $t_{cut} = 4.77$ and $r_{max} = 1044.6$. Again, the value of the elimination constant obtained here (0.230) is in excellent agreement with the one that describes the linear portion of the elimination (5–16 h) for the immediate-release tablet (0.225, $n = 7$, $r^2 = 0.99$) or the extended-release formulations. Values obtained for the time delay ($0.50/0.58 = 0.86$ h) and cut-off (4.77 h) are also very realistic. Again, incorporation of a second compartment provided no significant improvement with realistic parameters.

Plasma concentrations calculated with this common, fitted model (Figure 5) are sufficiently good; the slow formulation is somewhat underestimated. Predictions obtained by using the leave-one-out procedure are much less satisfactory, but they are not entirely unrealistic. A main reason for the poor fit is that the limiting absorption value is essentially needed only for the fast formulation (and to a small degree for the medium formulation); therefore, if only two formulations are used for the fitting, the obtained value may not be adequate for the third formulation. Except for the fast and medium formulation fitted with the common model, percent errors in fitted or predicted AUCs fail the required guidelines. Nevertheless, considering the problems related to the in-vivo absorption of metformin and the fact that no true IVIVC could be developed in the previous work, the obtained results already clearly illustrate the possibilities inherent to the present IVIVC method. The metformin data were included here to illustrate the capability of the present model to reasonably accommodate even compounds where other IVIVC methods could not be developed by relying only on a restricted number of meaningful adjustable

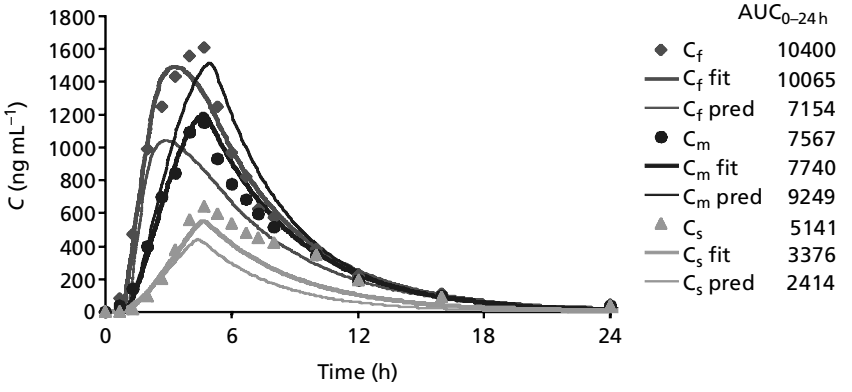

Figure 5 Plasma concentration–time profiles for the metformin data. C_f, C_m and C_s denote values for the fast-, medium- and slow-release formulations, respectively. Experimental data are shown together with predicted values from the present IVIVC method. Thicker lines (C fit) denote predictions of the model fitted simultaneously on all three formulations ($k = 0.230$, $s_r = 20.49$, $s_l = 0.58$, $t_0 = -0.50$, $t_{cut} = 4.77$ and $r_{max} = 1044.6$), and thinner lines (C pred) denote predicted values for each formulation by the model fitted on the other two formulations (leave-one-out predictions).

parameters. Because this differential-equation-based method allows for considerable modelling flexibility while still using a relatively limited number of parameters, it can be particularly useful in more complex cases. For example, if multiple plasma concentration peaks are present, such as in the glibenclamide data of Balan and co-workers (Balan et al 2000) or in the paracetamol data of Dalton and co-workers (Dalton et al 2001), they can be accounted for by inclusion of a more complex absorption profile in φ_{abs} or even by incorporation of enterohepatic recycling models (Roberts et al 2002; Wajima et al 2002).

Conclusions

Because in the present IVIVC model differential equations are directly integrated and no convolution or deconvolution techniques are used, various functional dependencies (e.g., time scaling) can be easily introduced to describe or to connect dissolution and absorption profiles. This can provide improved performance and increased modeling flexibility. Because of the transparent and pharmacokinetic-based nature of the model, it is also easy to interpret and cross-validate the parameter-values obtained. Furthermore, functions accounting for the variability of absorption conditions as the drug moves along the gastrointestinal tract can also be incorporated, and for the data sets explored here, even simple step-down functions provided significant improvement.

References

Agoram, B., Woltosz, W. S., Bolger, M. B. (2001) Predicting the impact of physiological and biochemical processes on oral drug bioavailability. *Adv. Drug Deliv. Rev.* **50** (Suppl 1): S41–S67

Amidon, G. L., Lennernas, H., Shah, V. P., Crison, J. R. (1995) A theoretical basis for a biopharmaceutic drug classification: the correlation of *in vitro* drug product dissolution and *in vivo* bioavailability. *Pharm. Res.* **12**: 413–420

Balan, G., Timmins, P., Greene, D. S., Marathe, P. H. (2000) In-vitro in-vivo correlation models for glibenclamide after administration of metformin/glibenclamide tablets to healthy human volunteers. *J. Pharm. Pharmacol.* **52**: 831–838

Balan, G., Timmins, P., Greene, D. S., Marathe, P. H. (2001) *In vitro-in vivo* correlation (IVIVC) models for metformin after administration of modified-release (MR) oral dosage forms to healthy human volunteers. *J. Pharm. Sci.* **90**: 1176–1185

Brockmeier, D., Dengler, H. J., Voegele, D. (1985) *In vitro-in vivo* correlation of dissolution,a time scaling problem? Transformation of *in vitro* results to the *in vivo* situation, using theophylline as a practical example. *Eur. J. Clin. Pharmacol.* **28**: 291–300

Buchwald, P. (2002) Complexation thermodynamics of cyclodextrins in the framework of a molecular size-based model for nonassociative organic liquids that includes a modified hydration-shell hydrogen-bond model for water. *J. Phys. Chem. B* **106**: 6864–6870

Buchwald, P., Bodor, N. (1999) Quantitative structure-metabolism relationships: steric and nonsteric effects in the enzymatic hydrolysis of noncongener carboxylic esters. *J. Med. Chem.* **42**: 5160–5168

Buchwald, P., Bodor, N. (2000) Simple model for nonassociative organic liquids and water. *J. Am. Chem. Soc.* **122**: 10671–10679

Buchwald, P., Bodor, N. (2001) A simple, predictive, structure-based skin permeability model. *J. Pharm. Pharmacol.* **53**: 1087–1098

Costa, P., Lobo, J. M. S. (2001) Modeling and comparison of dissolution profiles. *Eur. J. Pharm. Sci.* **13**: 123–133

Dalton, J. T., Straughn, A. B., Dickason, D. A., Grandolfi, G. P. (2001) Predictive ability of level A *in vitro-in vivo* correlation for RingCap controlled-release acetaminophen tablets. *Pharm. Res.* **18**: 1729–1734

Davis, S. S., Hardy, J. G., Fara, J. W. (1986) Transit of pharmaceutical dosage forms through the small intestine. *Gut* **27**: 886–892

Easton, D. M. (2002) Gompertz pharmacokinetic model for drug disposition. *Pharm. Res.* **19**: 463–469

Eddington, N. D., Marroum, P., Uppoor, R., Hussain, A., Augsburger, L. (1998) Development and internal validation of an *in vitro-in vivo* correlation for a hydrophilic metoprolol tartrate extended release tablet formulation. *Pharm. Res.* **15**: 466–473

Gabrielsson, J., Weiner, D. (2000) *Pharmacokinetic/pharmacodynamic data analysis: concepts and applications*. 3rd edn, Apotekarsocieteten (Swedish Pharmaceutical Press), Stockholm

Gibaldi, M., Perrier, D. (1982) *Pharmacokinetics*. 2nd edn, Marcel Dekker, New York

Gillespie, W. R. (1997) Convolution-based approaches for *in vivo-in vitro* correlation modeling. In: Young, D., Devane, J. G., Butler, J. (eds) *In vitro-in vivo correlations. Advances in experimental medicine and biology*. Vol. 423, Plenum, New York, pp 53–65

Gomeni, R., D'Angeli, C., Bye, A. (2002) *In silico* prediction of optimal *in vivo* delivery properties using convolution-based model and clinical trial simulation. *Pharm. Res.* **19**: 99–103

Langenbucher, F. (2002) Handling of computational in vitro/in vivo correlation problems by Microsoft Excel: I. Principles and some general algorithms. *Eur. J. Pharm. Biopharm.* **53**: 1–7

Loo, J. C. K., Riegelman, S. (1968) New method for calculating the intrinsic absorption rate of drugs. *J. Pharm. Sci.* **57**: 918–928

Modi, N. B., Lam, A., Lindemulder, E., Wang, B., Gupta, S. K. (2000) Application of *in vitro-in vivo* correlations (IVIVC) in setting formulation release specifications. *Biopharm. Drug Dispos.* **21**: 321–326

O'Hara, T., Hayes, S., Davis, J., Devane, J., Smart, T., Dunne, A. (2001) *In vivo-in vitro* correlation (IVIVC) modeling incorporating a convolution step. *J. Pharmacokinet. Pharmacodyn.* **28**: 277–298

Pitsiu, M., Sathyan, G., Gupta, S., Verotta, D. (2001) A semiparametric deconvolution model to establish in vivo-in vitro correlation applied to OROS oxybutynin. *J. Pharm. Sci.* **90**: 702–712

Riley, K. F., Hobson, M. P., Bence, S. J. (1997) *Mathematical methods for physics and engineering. A comprehensive guide*. Cambridge University Press, Cambridge

Roberts, M. S., Magnusson, B. M., Burczynski, F. J., Weiss, M. (2002) Enterohepatic circulation: physiological, pharmacokinetic and clinical implications. *Clin. Pharmacokinet.* **41**: 751–790

Sathe, P., Tsong, Y., Shah, V. P. (1997) *In vitro* dissolution profile comparison and IVIVR. In: Young, D., Devane, J. G., Butler, J. (eds) *In vitro-in vivo correlations. Advances in experimental medicine and biology*. Vol. 423, Plenum, New York, pp 31–42

Sirisuth, N., Eddington, N. D. (2000) Influence of stereoselective pharmacokinetics in the development and predictability of an IVIVC for the enantiomers of metoprolol tartrate. *Pharm. Res.* **17**: 1019–1025

US Department of Health and Human Services, Food and Drug Administration, Center for Drug Evaluation and

Research (CDER) (1997) *Guidance for industry. Extended release oral dosage forms: development, evaluation, and application of in vitro/in vivo correlations*. Rockville, MD

Veng-Pedersen, P., Gobburu, J. V. S., Meyer, M. C., Straughn, A. B. (2000) Carbamazepine level-A in vivo-in vitro correlation (IVIVC): a scaled convolution based predictive approach. *Biopharm. Drug Dispos.* **21**: 1–6

Vidon, N., Chaussade, S., Noel, M., Franchisseur, C., Huchet, B., Bernier, J. J. (1988) Metformin in the digestive tract. *Diabetes Res. Clin. Pract.* **4**: 223–229

Wagner, J. G. (1975) *Fundamentals of clinical pharmacokinetics*. Drug Intelligence Publications, Hamilton, IL

Wagner, J. G., Nelson, E. (1963) Percent absorbed time plots derived from blood level and/or urinary excretion data. *J. Pharm. Sci.* **52**: 610–611

Wajima, T., Yano, Y., Oguma, T. (2002) A pharmacokinetic model for analysis of drug disposition profiles undergoing enterohepatic circulation. *J. Pharm. Pharmacol.* **54**: 929–934

Wang, Y., Nedelman, J. (2002) Bias in the Wagner-Nelson estimate of the fraction of drug absorbed. *Pharm. Res.* **19**: 470–476

Wilding, I. (2000) Site-specific drug delivery in the gastrointestinal tract. *Crit. Rev. Ther. Drug Carrier Syst.* **17**: 557–620

Yu, L. X., Amidon, G. L. (1999) A compartmental absorption and transit model for estimating oral drug absorption. *Int. J. Pharm.* **186**: 119–125

Appendix 1 Scientist model file for the present IVIVC model

```
// MicroMath Scientist Model File
// IVIVC diff. eq. model for sigmoidal (n, t50, fmax = 100) dissolution profiles
// One compartment (k), time-scaling (s1), time-shift (t0), and sigmoidal step-down cut-off (tcut)
// Simultaneous fit on three different formulations (c1, c2, c3)
// Peter Buchwald, 2002
Independent Variable(s): t
Dependent Variable(s): c1, c2, c3
Parameter(s): k, sr, s1, t0, tcut
fmax = 100
t50_1 = 1.6054
n1 = 1.8500
t50_2 = 3.628
n2 = 1.522
t50_3 = 6.406934
n3 = 2.4420
eta = 10
phi = exp(-eta*(t-tcut))/(1 + exp(-eta*(t-tcut)))
C1' = ifgezero(t0+s1*t,phi*sr*n1*fmax*t50_1^n1*(t0+s1*t)^(n1-1)/(t50_1^n1+(t0+s1*t)^n1)^2-k*C1,0)
C2' = ifgezero(t0+s1*t,phi*sr*n2*fmax*t50_2^n2*(t0+s1*t)^(n2-1)/(t50_2^n2+(t0+s1*t)^n2)^2-k*C2,0)
C3' = ifgezero(t0+s1*t,phi*sr*n3*fmax*t50_3^n3*(t0+s1*t)^(n3-1)/(t50_3^n3+(t0+s1*t)^n3)^2-k*C3,0)
//initial conditions
t = 0
c1 = 0
c2 = 0
c3 = 0
***
```

Appendix 2 WinNonlin model file for the present IVIVC model

```
MODEL
remark WinNonlin model file
rema   IVIVC diff. eq. model for sigmoidal (n, t50, fmax = 100) dissolution profiles
rema   One compartment (k), time-scaling (s1), time-shift (t0),
rema       and sigmoidal step-down cut-off (tcut)
rema   Simultaneous fit on three different formulations (f 1, 2, 3)
rema   Peter Buchwald, 2002
rema
rema      no.     parameter     constant     secondary parm.
rema      ---     ---------     --------     ---------------
rema      1        sr              eta            k half life
rema      2        k               fmax
rema      3        s1              t50_1
rema      4        t0              n_1
rema      5        tcut            t50_2
rema      6                         n_2
rema      7                         t50_3
```

```
rema      8                          n_3
rema ************************************************
rema          i---------------------i
rema          i                     i
rema   r -->  i    compartment 1    i ---> k
rema  (IVIVC) i                     i
rema          i---------------------i
rema ************************************************
comm
nparm 5
pnames `sr', `k', `s1', `t0', `tcut'
ncons 8
nfunc 3
fnum 3
nsec 1
snames `k_hl'
nderivatives 3
end

temp
t = x
eta = con(1)
fmax = con(2)
t50_1 = con(3)
n_1 = con(4)
t50_2 = con(5)
n_2 = con(6)
t50_3 = con(7)
n_3 = con(8)
end

start
z(1) = 0
z(2) = 0
z(3) = 0
end

diff
phi = exp(-eta*(t-tcut))/(1 + exp(-eta*(t-tcut)))
if (t0 + s1*t)>0 then
dz(1) = phi*sr*n_1*fmax*t50_1**n_1*(t0 + s1*t)**(n_1-1)/(t50_1**n_1 + (t0 + s1*t)**n_1)**2 - k*z(1)
dz(2) = phi*sr*n_2*fmax*t50_2**n_2*(t0 + s1*t)**(n_2-1)/(t50_2**n_2 + (t0 + s1*t)**n_2)**2 - k*z(2)
dz(3) = phi*sr*n_3*fmax*t50_3**n_3*(t0 + s1*t)**(n_3-1)/(t50_3**n_3 + (t0 + s1*t)**n_3)**2 - k*z(3)
else
  dz(1) = 0
  dz(2) = 0
  dz(3) = 0
endif
end

func 1
f = z(1)
end

func 2
f = z(2)
end

func 3
f = z(3)
end

seco
k_hl = -dlog(.5)/k
end

EOM
```